

# The combination of pulsed acousto-optic imaging and *B*-mode diagnostic ultrasound for three-dimensional imaging in *ex vivo* biological tissue

Lei Sui<sup>\*</sup>, Todd W. Murray<sup>†</sup>, and Ronald A. Roy<sup>‡</sup>

Department of Aerospace and Mechanical Engineering, Boston University,  
110 Cummings Street, Boston, MA, 02215

## ABSTRACT

A multimode imaging system, producing conventional ultrasound (US) and acousto-optic (AO) images, has been developed and used to detect optical absorbers buried in excised biological tissue. A commercially-available diagnostic ultrasound imaging transducer is used to both generate *B*-mode ultrasound images and as a pump for AO imaging. Due to the fact that the steered and focused beam used for US imaging and the US source for pumping the AO image are generated from the same ultrasound probe, the acoustical and optical images are intrinsically co-registered. AO imaging is performed using short ultrasound pulse trains at a frequency of 5 MHz. The phase-modulated light emitted from the interaction region is detected using a photorefractive-crystal based interferometry system. Experimental results have previously been presented for the two-dimensional imaging in tissue-mimicking phantoms. In this paper, we report further experimental developments demonstrating three-dimensional fusion of *B*-mode ultrasound imaging and pulsed acousto-optic imaging in excised biological tissue (~2 cm thick). By mechanically scanning the ultrasound transducer array in a direction perpendicular to its imaging plane, both the acoustical and optical properties of an embedded target are obtained in three dimensions. The results suggest that AO imaging could be used to supplement conventional *B*-mode ultrasound imaging with optical contrast, and the multimode imaging system may find application in the detection and diagnosis of cancer.

Keywords: Pulsed acousto-optic imaging, *B*-mode diagnostic ultrasound, multimode, three-dimensional imaging, photorefractive crystal, biological tissue

## 1. INTRODUCTION

Acousto-optic imaging (AOI) in optically diffuse media has received considerable attention in recent years.<sup>1-33</sup> In this technique, photons are modulated or tagged within the sample using a focused ultrasound beam,<sup>2,3,5,14</sup> and detection of this modulated light gives a measure of the subsurface light distribution in the interaction region. The motivation for developing such systems is to measure optical properties at relatively large depths within biological tissue with high spatial resolution. AOI allows for optical contrast mapping in turbid media with resolution approaching that of ultrasound imaging.

We have recently developed a photorefractive crystal based interferometer with sufficient sensitivity to detect acousto-optic signals produced using a pulsed ultrasonic source.<sup>23,26,28,29</sup> In addition, we have used a conventional US imaging system to pump the AO response, allowing for co-registered AO and conventional US images to be obtained.<sup>30</sup> Our primary motivation for developing such a multimode imaging system is to supplement the information obtained from conventional ultrasound with additional AO information. Ultimately, this may lead to an improvement in the specificity of breast cancer detection and diagnosis over what has thus far been demonstrated using ultrasound alone. Leveque-Fort *et al.* originally proposed the combination of AOI with ultrasound, and used CW ultrasound to pump the AO response.<sup>11</sup>

---

<sup>\*</sup> Lei Sui, Email: [suilei@bu.edu](mailto:suilei@bu.edu); Phone: 617-353-7366;

<sup>†</sup> Todd W. Murray, Email: [twmurray@bu.edu](mailto:twmurray@bu.edu); Phone: 617-353-3951;

<sup>‡</sup> Ronald A. Roy, Email: [ronroy@bu.edu](mailto:ronroy@bu.edu); Phone: 617-353-4846.

More recently, we have presented 2D AO/US imaging results in polyacrylamide gel tissue phantoms using a conventional US transducer operating in pulsed mode to pump the AO response.<sup>30</sup> In this paper, we present experimental results demonstrating 3D US/AO imaging using pulsed ultrasound in thick ( $\sim 2$  cm) excised chicken breast.

## 2. EXPERIMENTAL SETUP

The experimental setup is shown in Fig. 1. A 230 mW frequency doubled Nd:YAG laser (532 nm) source is sent to a variable beam splitter where it is split into signal and reference beams with a power ratio of approximately 40:1. The reference beam is directed around the test tank and sent to a BSO photorefractive crystal. The signal beam is expanded to a diameter of approximately 2 cm and delivered to the submerged sample. The resulting power density at the sample surface is about  $62\text{mW}/\text{cm}^2$ , which is well below the safety limit.<sup>34</sup> The scattered light is collected by a lens and mixed with the reference beam in the BSO crystal. The APD output is amplified, low-pass filtered at 500 kHz, and sent to a digital storage oscilloscope. Details of the AOI signal detection using the PRC based interferometry have been presented elsewhere.<sup>23,26,28,33</sup> A commercially available ultrasound probe (192-element 5 MHz linear array, type 8802, B&K Medical, Herlev, Denmark) is excited in pulsed mode by a PC based diagnostic ultrasound imaging machine (AN2300, Analogic Corp., Peabody, MA, USA).

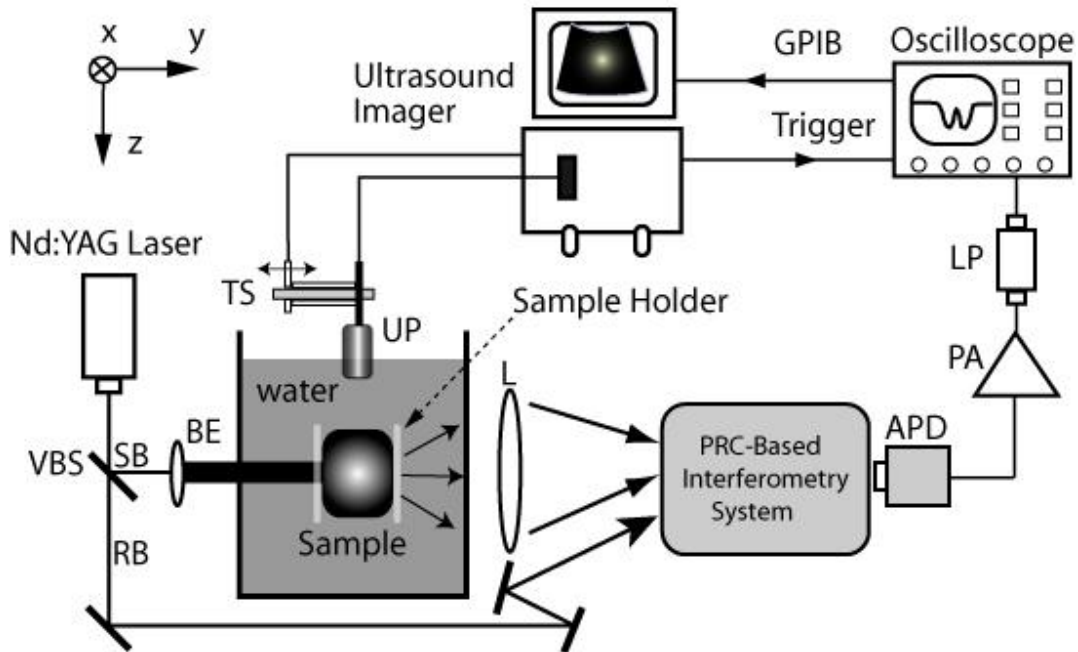


Figure 1. The experimental setup with the following labels: VBS: variable beam splitter, RB: reference beam, SB: signal beam, BE: beam expander, UP: ultrasound probe, TS: translation stages, APD: avalanche photodiode, PA: preamplifier, LP: low pass filter.

A chicken breast sample is placed between two parallel, transparent plastic plates of 1.3 mm thickness, with the sample oriented such that the plate walls are perpendicular to the optical axis. The dimensions of the sample, after mounting, are  $\sim 4.5\text{cm} \times 2\text{cm} \times 4.5\text{cm}$  along the X, Y and Z axes, respectively (see the reference coordinate system given in Fig. 1). Both the sample and the ultrasound probe are submerged in a glass tank ( $30\text{cm} \times 30\text{cm} \times 20\text{cm}$  along the X, Y and Z axes, respectively) filled with degassed and filtered water. Prior to mounting, a cut was made midway through the breast across the X-Z plane and a 4 mm cube of poly-acrylamide gel, doped with India ink to give an absorption coefficient  $3\text{ cm}^{-1}$ , was inserted. This procedure was performed while the sample was submerged in degassed water to minimize the

possibility of trapping gas bubbles. The gel target has a sound speed of  $1.515 \text{ mm}/\mu\text{s}$  and a bulk density of  $1.05 \text{ mg}/\text{mm}^3$ . A cut-away view of the chicken breast sample along with the embedded gel target is shown in Fig. 2 (a).

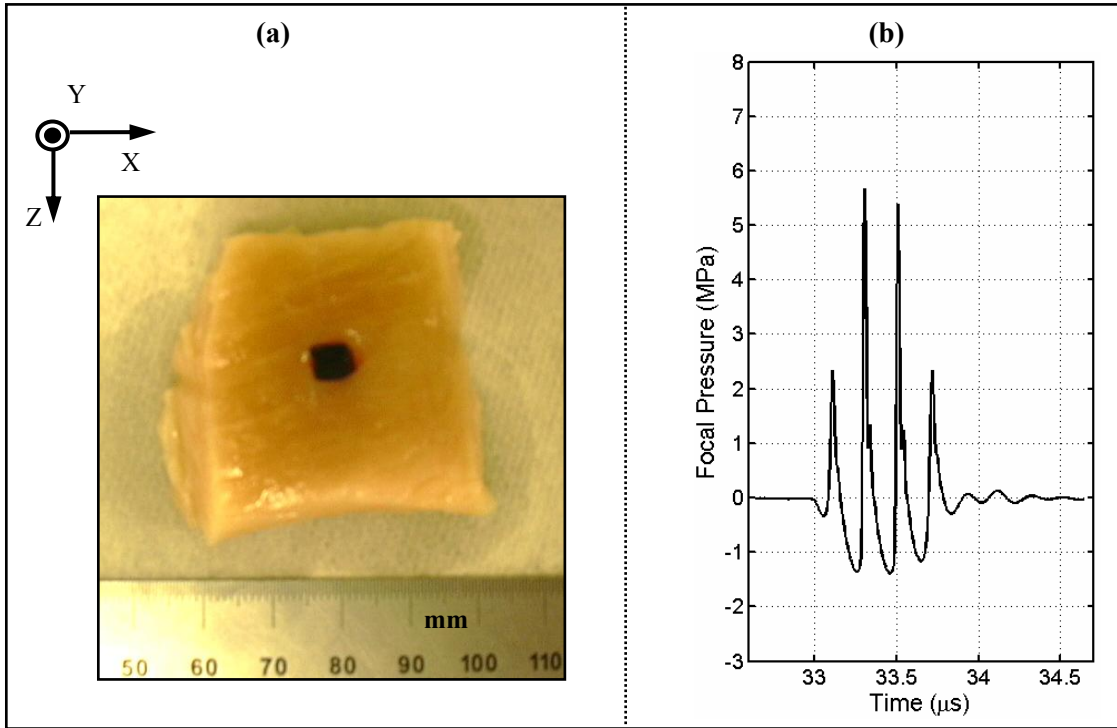


Figure 2. (a) A cut-away view of the chicken breast sample ( $\sim 4.5 \times 4.5 \times 2 \text{ cm}^3$  along the X, Z, Y directions, respectively) with an optically absorbing target ( $4 \times 4 \times 4 \text{ mm}^3$ ). The target was made of poly-acrylamide gel (see Ref. 23 for details) with India ink added; (b) A 3-cycle pulse measured at the focal spot of the ultrasound probe.

In order to obtain US and AO images, the probe is centered on the sample such that the imaging plane coincides with the X-Z plane. Starting at a given Y location of the probe, ultrasound pulses are electronically steered to fire along different directions in a fan-like pattern originating from the geometric center of the transducer, with the ultrasound focal length fixed at 50 mm. This technique yields the standard *B*-mode backscattered ultrasound image, and by monitoring the AO signal as a function of time, the acousto-optic response of the tissue is also measured along each scan line. The AO scans employ either 3-cycle or 9-cycle ultrasound pulses with a center frequency of 5 MHz. A typical 3-cycle ultrasound pulse measured in water at the focal spot of the ultrasound probe is shown in Fig. 2 (b), where the distortion of the waveform is caused by the nonlinear propagation. The spatial peak acoustic pressure amplitude is approximately 1.4 MPa peak-negative and 5.7 MPa peak-positive. The pulse repetition frequency is 1 kHz and the AO signal along each line is averaged 40,000 and 10,000 times for 3-cycle and 9-cycle pulses, respectively. A total of 192 scan lines form a *B*-mode ultrasound image. Both the AO signals and ultrasound echoes are digitized in the time domain and converted to the space domain using a sound speed of  $1.5 \text{ mm}/\mu\text{s}$ . Once the AO/US images are acquired, the ultrasonic probe is mechanically scanned to the next position along the Y axis and the scanning procedure is repeated.

### 3. EXPERIMENTAL RESULTS AND DISCUSSION

Figure 3 (a) shows normalized AO signals resulting from individual 3-cycle scan lines fired along the Z axis. Plot (2) corresponds to the scan that traverses the center of the target at  $Y=0$ , and plots (1) and (3) correspond to the scans made 6 mm before and after the center of the target, as shown in Fig. 3 (b). The strength of the AO signal, for a given US pump source, provides a measure of the photon density in the region where the light and sound interact. In the cases where the US does not intersect the target, the negative going AO signal profile tracks the distribution of background diffuse light within the sample. When the ultrasound does intersect the optically absorbing target, however, the total

amount of modulated light reaching the detector reduces, leading to the peak (positive going) in the center of the AO signal observed at position 2. The SNR of the signal observed at position 1 is somewhat higher than that observed at position 3 due to the greater amount of photons modulated when the ultrasound probe is closer to the incident laser beam.<sup>33</sup>

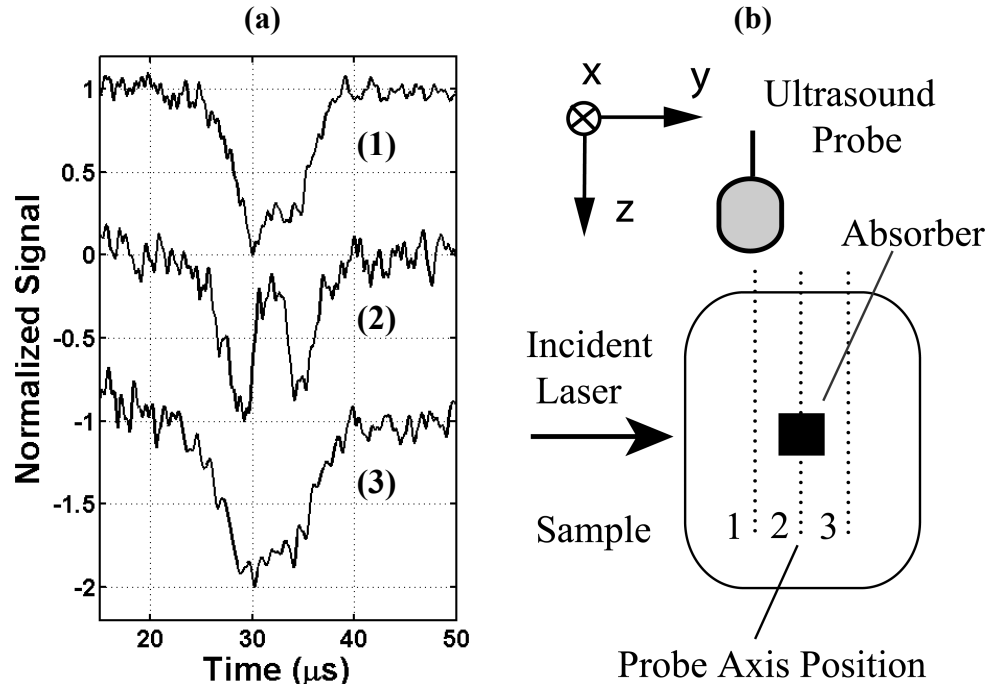


Figure 3. The normalized AO signals (a) detected when the ultrasound probe is scanned along the Y axis at 3 different locations corresponding to: position 1, 2 and 3 as depicted in (b). Note that trace (1) and trace (3) in (a) have been offset from 0 for display purposes and position 1, 2 and 3 in (b) are separated by 6 mm along the Y axis with position 2 right crossing the center of the target.

Figure 4 shows a series of XZ-plane AO images at several different Y positions within the sample, with  $Y=0$  corresponding roughly to the center of the inclusion. The signals have been processed to remove the AO signal contribution from the background diffuse light distribution using the following procedure. First, the raw data is smoothed using adjacent averaging (roughly equivalent to low-pass filtering at 625 kHz). The data is then fit to a Gaussian function, using only the portions of the signal that precede and follow the region where the inclusion is expected. This provides an estimate of the background light distribution, in the absence of the optical absorber. By subtracting this estimate from the measured AO response, and subsequently normalizing the response to the background light level, we obtain the AO response produced by the presence of the optical inhomogeneity. This operation is repeated for each scan line and the resulting signal levels are converted to a color scale, resulting in the images shown in Fig. 4. For this experiment, a 9-cycle ultrasound pulse with a spatial pulse length of 2.7 mm was used to pump the AO interaction. A longer pulse length allows for improved SNR by increasing the sound and light interaction volume, but this comes at the expense of axial resolution.<sup>33</sup> The target is clearly observed and localized in three dimensions. It is important to point out that the contrast in the AO images is not a direct measure of the distribution of optical absorption within the sample, but rather it depends on both the photon distribution in the light/sound interaction region, and the probability that the modulated photons will be received by the detection system.<sup>33</sup> These parameters, in turn, depend on the characteristics of the source and detection system and the spatial distribution of optical properties. Three-dimensional AO images can potentially be used to determine the quantitative optical absorption or scattering distribution through the use of an inversion algorithm similar to those currently employed for diffuse optical tomography. Returning to Fig. 4, there are faint indications of the absorber when the ultrasound scan plane is before ( $Y = -4.0$  mm) and after ( $Y = 6$  mm) the actual target. This may be due to changes in the local photon distribution near

the target surface, or a shadowing effect where the presence of the target reduces the probability that modulated photons will be detected.

Line scans taken through the center of the target along the X, Y, and Z directions using 3-cycle ultrasonic pulses show that the apparent size of the imaged inclusion is comparable to the actual size of the embedded target in the X and Z directions, and the image resolution, taken as the distance required for the signal to increase from 10% to 90% of the peak value, is approximately 2 mm in both X and Z. The resolution along the Y-direction is estimated to be approximately 3mm, somewhat broader than that observed along X and Z.

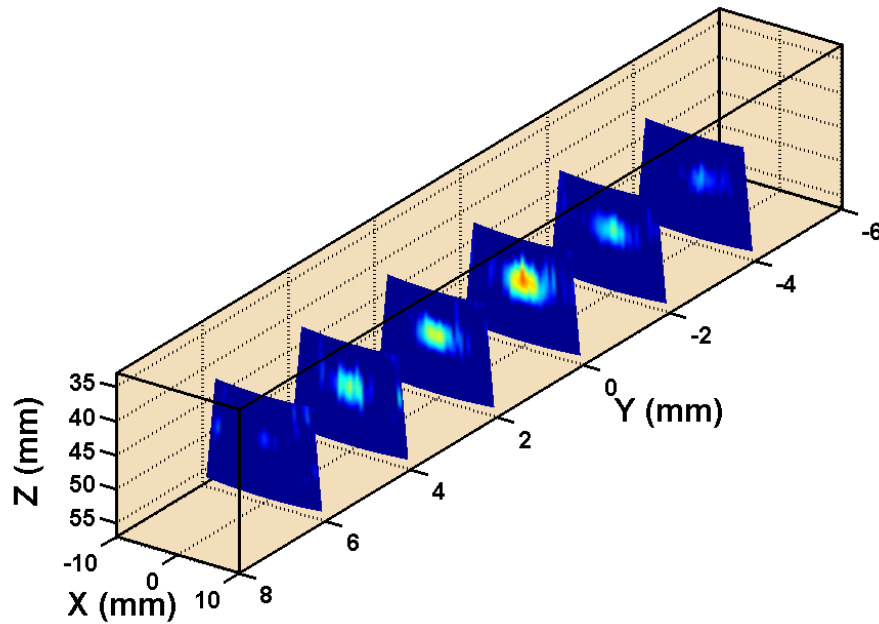


Figure 4. Acousto-optic images of the embedded target obtained by mechanically scanning the probe along Y axis.

#### 4. CONCLUSIONS

In summary, we have demonstrated US/AO imaging *ex vivo* in 2-cm thick chicken breast with an embedded optically absorbing inclusion. We have also demonstrated that 3-D maps of the AO response can be obtained by scanning the US probe in one dimension, and that spatial resolution on the order of 2-3 mm is possible in all three directions. It is important to note that these results were obtained using a wavelength of 532 nm, and significant improvements in SNR are anticipated by moving to the NIR wavelength range. The response time of the PRC used in these experiments is approximately 150 ms under our experimental conditions. This is not suitable for *in vivo* imaging where the speckle decorrelation time has been measured to be on the order of 1 ms.<sup>20,32</sup> However, the PRC detection approach presented here can be applied in the NIR wavelength band where semiconductor photorefractives possessing response times in the desired range are available.

#### ACKNOWLEDGEMENT

The authors would like to acknowledge Prof. Charles A. DiMarzio for valuable discussions, and Dr. Emmanuel Bossy for his assistance in setting up the ultrasound instrumentation. This work was supported in part by CenSSIS, *the Center*

for *Subsurface Sensing and Imaging Systems*, under the Engineering Research Centers Program of the National Science Foundation (award number EEC-9986821).

## REFERENCES

1. D. Dolfi and F. Micheron, "Imaging process and system for transillumination with photon frequency marking," International Patent WO 89/00278 (1989).
2. F. A. Marks, H. W. Tomlinson, and G. W. Brooksby, "A comprehensive approach to breast cancer detection using light: photon localization by ultrasound modulation and tissue characterization by spectral discrimination," in *Photon Migration and Imaging in Random Media and Tissues*, B. Chance and R. R. Alfano, eds., Proc. SPIE **1888**, 500-510 (1993).
3. W. Leutz and G. Maret, "Ultrasonic modulation of multiply scattered light," *Physica B* **204**, 14-19 (1995).
4. L.-H. Wang, S. L. Jacques, and X.-M. Zhao, "Continuous-wave ultrasonic modulation of scattered laser light to image objects in turbid media," *Opt. Lett.* **20**, 629-631 (1995).
5. M. Kempe, M. Larionov, D. Zaslavsky, and A. Z. Genack, "Acousto-optical tomography with multiply scattered light," *J. Opt. Soc. Am. A* **14**, 1151-1158 (1997).
6. L.-H. Wang and G. Ku, "Frequency-swept ultrasound-modulated optical tomography of scattering media," *Opt. Lett.* **23**, 975-977 (1998).
7. G. D. Mahan, W. E. Engler, J. J. Tiemann and E. Uzgiris, "Ultrasonic tagging of light: Theory," *Proc. Natl. Acad. Sci. USA* **95**, 14015-14019 (1998).
8. S. Leveque, A. C. Boccara, M. Lebec, and H. Saint-Jalmes, "Ultrasonic tagging of photon paths in scattering media: parallel speckle modulation processing," *Opt. Lett.* **24**, 181-183 (1999).
9. G. Yao, S. Jiao and L.V. Wang, "Frequency-swept ultrasound-modulated optical tomography in biological tissue by use of parallel detection," *Opt. Lett.* **25**, 734-736 (2000).
10. A. Lev, Z. Kotler and B. G. Sfez, "Ultrasound tagged light imaging in turbid media in a reflectance geometry," *Opt. Lett.* **25**, 378-380 (2000).
11. S. Leveque-Fort, J. Selb, L. Pottier, and A. C. Boccara, "Setup for simultaneous imaging of optical and acoustic contrasts in biological tissues," *Proc. SPIE* **4256**, 200-206 (2001).
12. S. Leveque-Fort, "Three-dimensional acousto-optic imaging in biological tissues with parallel signal processing," *Appl. Opt.* **40**, 1029-1036 (2001).
13. S. Leveque-Fort, J. Selb, L. Pottier and A. C. Boccara, "In situ local tissue characterization and imaging by backscattering acousto-optic imaging," *Opt. Comm.* **196**, 127-131 (2001).
14. L.-H. Wang, "Mechanisms of ultrasonic modulation of multiply scattered coherent light: an analytic model," *Phys. Rev. Lett.* **87**, 043903(1-4) (2001).
15. A. Lev and B. G. Sfez, "Direct, noninvasive detection of photon density in turbid media," *Opt. Lett.* **27**, 473-475 (2002).
16. J. Selb, L. Pottier, and A. C. Boccara, "Nonlinear effects in acousto-optic imaging," *Opt. Lett.* **27**, 918-920 (2002).
17. M. Gross, P. Goy and M. Al-Koussa, "Shot-noise detection of ultrasound-tagged photons in ultrasound-modulated optical imaging," *Opt. Lett.* **28**, 2482-2484 (2003).
18. B. C. Forget, F. Ramaz, M. Atlan, J. Selb, and A. C. Boccara, "High-contrast fast Fourier transform acousto-optical tomography of phantom tissues with a frequency-chirp modulation of the ultrasound," *Appl. Opt.* **42**, 1379-1383 (2003).
19. A. Lev and B. G. Sfez, "Pulsed ultrasound-modulated light tomography," *Opt. Lett.* **28**, 1549-1551 (2003).
20. A. Lev, and B. Sfez, "In vivo demonstration of the ultrasound-modulated light technique," *J. Opt. Soc. Am. A* **20**, 2347-2354 (2003).
21. L. -H. Wang, "Ultrasound-mediated biophotonic imaging: A review of acousto-optical tomography and photo-acoustic tomography," *Dis. Markers* **19**, 123-138 (2003).
22. J. Li, S. Sakadzic, G. Ku and L. H. V. Wang, "Transmission- and side-detection configurations in ultrasound-modulated optical tomography of thick biological tissues," *Appl. Opt.* **42**, 4088-4094 (2003).

23. L. Sui, T. Murray, G. Maguluri, A. Nieva, F. Blonigen, C. DiMarzio and R. A. Roy, "Enhanced detection of acousto-photon scattering using a photorefractive crystal," in *Photons Plus Ultrasound: Imaging and Sensing*, A. A. Oraevsky and L. V. Wang, eds., Proc. SPIE **5320**, 164-171 (2004).
24. J. Li and L. V. Wang, "Ultrasound-modulated optical computed tomography of biological tissues", *Appl. Phys. Lett.* **84**, 1597-1599 (2004).
25. F. Ramaz, B.C. Forget, M. Atlan, A.C. Boccara, M. Gross, P. Delaye, and G. Roosen, "Photorefractive detection of tagged photons in ultrasound modulated optical tomography of thick biological tissues," *Opt. Express* **12**, 5469-5474 (2004).
26. T. W. Murray, L. Sui, G. Maguluri, R. A. Roy, A. Nieva, F. Blonigen, and C. A. DiMarzio, "Detection of ultrasound-modulated photons in diffuse media using the photorefractive effect," *Opt. Lett.* **29**, 2509-2511 (2004).
27. S. Sakadzic and L. V. Wang, "High-resolution ultrasound-modulated optical tomography in biological tissues," *Opt. Lett.* **29**, 2770-2772 (2004).
28. L. Sui, R. A. Roy, C. A. DiMarzio, and T. W. Murray, "Imaging in diffuse media using pulsed-ultrasound-modulated light and the photorefractive effect," *Appl. Opt.* **44**, 4041-4048 (2005).
29. L. Sui., R. A. Roy, C. A. DiMarzio, F. Blonigen and T. W. Murray, "Investigation of the photorefractive crystal based detection system for acousto-optical imaging (AOI) in highly diffuse media," in *Photons Plus Ultrasound: Imaging and Sensing 2005*, A. A. Oraevsky and L. H. Wang, eds., Proc. SPIE **5697**, 136-144 (2005).
30. E. Bossy, L. Sui, T. W. Murray, and R. A. Roy, "Fusion of conventional ultrasound imaging and acousto-optic sensing (AOS) by use of a standard pulsed-ultrasound scanner," *Opt. Lett.* **30**, 744-746 (2005).
31. M. Atlan, B. C. Forget, F. Ramaz, A. C. Boccara, and M. Gross, "Pulsed acousto-optic imaging in dynamic scattering media with heterodyne parallel speckle detection," *Opt. Lett.* **30**, 1360-1362 (2005).
32. M. Gross, P. Goy, B. C. Forget, M. Atlan, F. Ramaz, A. C. Boccara, and A. K. Dunn, "Heterodyne detection of multiply scattered monochromatic light with a multipixel detector," *Opt. Lett.* **30**, 1357-1359 (2005).
33. L. Sui, "Acousto-optic imaging in diffuse media using pulsed ultrasound and the photorefractive effect," Ph. D. Thesis, Boston University (2006).
34. American National Standards Institute, American National Standard for the Safe Use of Lasers in Health Care Facilities. Standard Z136.1-2000 (ANSI, Inc., New York) (2000).